BIOLOGY OF REPRODUCTION **66,** 843–855 (2002)

KRP3A and KRP3B: Candidate Motors in Spermatid Maturation in the Seminiferous Epithelium[1]

Yong Zou,[3] Clarke F. Millette,[4] and Ann O. Sperry[2,3]

Department of Anatomy and Cell Biology,[3] Brody School of Medicine at East Carolina University, Greenville, North Carolina 27858
Department of Cell Biology and Neuroscience,[4] University of South Carolina School of Medicine, Columbia, South Carolina 29209

ABSTRACT

We have identified KRP3, a novel kinesin-related protein expressed in the mammalian testis, and have examined the tissue distribution and subcellular localization of isoforms of this protein. Isolation of KRP3 clones, using the head domain identified in a previous PCR screen as probe, identified at least two KRP3 isoforms in the rat. We have isolated coding sequences of two highly related cDNAs from the rat testis that we have termed KRP3A and KRP3B (kinesin-related protein 3, A and B). Both cDNAs code for predicted polypeptides with the three-domain structure typical of kinesin superfamily members; namely a conserved motor domain, a region capable of forming a limited coiled-coil secondary structure, and a globular tail domain. Although almost identical in their head and stalk domains, these motors diverge in their tail domains. This group of motors is found in many tissues and cell types. The KRP3B motor contains DNA-binding motifs and an RCC1 (regulator of chromosome condensation 1) consensus sequence in its tail domain. Despite this similarity, KRP3B is not associated with the same structures as RCC1. Instead, KRP3 isoforms localize with the nuclei of developing spermatids, and their immunolocalization in the testis overlaps with that of the small GTPase Ran. Like Ran, KRP3 motors are associated in a polarized fashion with the nucleus of maturing spermatids at various stages of elongation. Our findings suggest a possible role for KRP3 motor isoforms in spermatid maturation mediated by possible interaction with the Ran GTPase.

gamete biology, gametogenesis, sperm maturation, spermatid, testis

INTRODUCTION

Successful spermatogenesis requires the participation of two principal cell types within the seminiferous epithelium; the gametogenic cells, and the supporting Sertoli cells. Each of these cell types contains an abundant and complex microtubule cytoskeleton that undergoes extensive rearrangement during the cycle of spermatogenesis. The microtubule network of a spermatogenic cell reorganizes during its lifetime to form the mitotic and meiotic spindles, the spermatid manchette, and the sperm flagella. The transformation of the Sertoli cell microtubule cytoskeleton is, perhaps, less dramatic but is no less important to its functions, including structural support of germ cells as well as positioning spermatids within the epithelium.

Molecular motors perform important functions in many types of intracellular motility and are specialized to perform tasks ranging from chromosome segregation to vesicle transport (reviewed in [1–3]). The cells of the seminiferous epithelium provide an excellent opportunity to examine the different structural demands on these specialized proteins in an array of microtubule complexes. Although microtubule-based movements are critical to spermatogenesis and Sertoli cell function, only a handful of motor proteins have been identified and characterized from the seminiferous epithelium [4–7].

To our knowledge, one class of kinesin-related molecular motors that has not been identified so far in the testis are those that associate with nuclei and/or DNA. Kinesins binding DNA have been identified with functions in metaphase chromosome alignment and nuclear architecture [8, 9]. The chromatin of spermatogenic cells undergoes extraordinary remodeling during the transformation to mature spermatozoa. This change involves the substitution of somatic histones sequentially with testis-specific histone variants, transition proteins, and finally, protamines. Concomitant with nuclear condensation is the radical reshaping of the spermatid nucleus. The molecular and regulatory mechanisms underlying these profound transformations in chromatin structure and nuclear shape are not completely understood. As the spermatid nuclear content and shape are drastically modified, the spermatids are transported through the epithelium by a proposed, microtubule-based mechanism [10].

The motor proteins described here are localized to the nucleus of developing male germ cells and are candidate motors involved in the morphological changes associated with spermatid maturation. In addition, we have localized RCC1 (regulator of chromosome condensation 1) to the manchette of condensing spermatids. The chromatin-bound exchange factor for the small GTPase Ran, RCC1 has been implicated along with Ran in such critical nuclear activities as nuclear-cytoplasmic transport, spindle nucleation, and nuclear membrane formation [11–13]. Ran itself is closely associated with KRP3 (kinesin-related protein 3) motors and the developing spermatid nucleus in a pivotal location for regulation of the nuclear transformations of spermatogenesis.

MATERIALS AND METHODS

Isolation and Characterization of cDNA Clones and DNA Manipulations

Recombinant lambda gt10 clones containing KRP3-related sequences were identified by hybridization screening of a rat testis library (Clontech, Palo Alto, CA) according to established techniques [6]. The two unique cDNA clones, termed KRP3A and KRP3B, were sequenced in both directions with overlapping oligonucleotide primers

[1]Supported in part by grants GM60628 (A.O.S.) and HD15269 and HD37280 (C.F.M.) from the National Institutes of Health.
[2]Correspondence: Ann O. Sperry, Dept. of Anatomy and Cell Biology, Brody School of Medicine at East Carolina University, 600 Moye Blvd., Greenville, NC 27858. FAX: 252 816 2850;
e-mail: sperrya@mail.ecu.edu

Received: 15 June 2001.
First decision: 16 July 2001.
Accepted: 31 October 2001.

ISSN: 0006-3363. http://www.biolreprod.org

(Gibco-BRL, Rockville, MD; the sequencing facility at the University of Tennessee, Knoxville). Sequence analysis was performed using Dnasis (Eastman Kodak, Rochester, NY), and alignments were generated against sequences in GenBank databases using the National Center for Biotechnology Information Blast server. The probability that regions of these proteins assume a coiled-coil structure was determined using the secondary-structure prediction programs Coils and Paircoils [14, 15].

In Situ Hybridization and Northern Blot Analysis

The KRP3 messages were detected with in situ hybridization (ISH) essentially as described previously [6] except using digoxigenin (DIG)-labeled probes instead of radioactive ones with modifications [16]. Testes were dissected from adult, prepuberal, or puberal rats and immersion-fixed overnight in 4% (w/v) paraformaldehyde (PFA) in PBS (pH 7.4) after piercing of the capsule at the poles and orbit. In some cases, testes were perfusion-fixed through the spermatic artery after removal from the animal. The organs were then incubated overnight in 0.5 M sucrose in PBS, placed in cryoprotectant, cut into 15-μm sections, and transferred to Vectabond-coated slides (Vector Laboratories, Burlingame, CA). After drying at 37°C, the sections were washed with PBS and treated with 0.3% Triton X-100 for 15 min at room temperature. Sections were washed again with PBS, digested with 1 μg/ml of proteinase K for 15 min at room temperature, and postfixed with 4% PFA in PBS for 5 min at room temperature. Sections were then acetylated, dehydrated, and prehybridized in 4× SSC (1× SSC: 0.15 M sodium chloride and 0.015 M sodium citrate) in 50% (v/v) deionized formamide at 37°C for 15 min.

Antisense RNA probes were prepared as described previously from linearized Bluescript vectors containing KRP fragments [6]. The following plasmids were used as template for transcription: 1) pKRP2, containing approximately 500 base pairs (bp) encoding the motor domain, 2) pKRP3, with approximately 500 bp encoding the KRP3 motor domain, 3) p72.1tail, containing 150 bp from the unique tail of KRP3A, and 4) p85.2tail, containing 450 bp from the unique tail of KRP3B. Plasmids were linearized with the appropriate enzyme, purified, and used as template for run-off transcription in the presence of DIG-labeled uridine triphosphate. The probe yield and DIG incorporation were quantified using test and control strips from Boehringer Mannheim (Indianapolis, IN). Sections were incubated with 5–10 ng of labeled probe in approximately 40 μl of hybridization solution (40% [v/v] deionized formamide, 10% [w/v] dextran sulfate, 1× Denhardt solution, 4× SSC, 10 mM dithiothreitol, 1 mg/ml of yeast tRNA, and 1 mg/ml of denatured and sheared salmon sperm DNA). Hybridization was conducted for a minimum of 16 h at 50°C under a coverglass sealed with rubber cement. After hybridization, sections were treated with RNase and rinsed with increasing stringency, concluding with two 10-min washes in 0.1× SSC at 45°C.

Labeled probe was localized with an alkaline phosphatase-conjugated anti-DIG antibody (Boehringer Mannheim) diluted 1:1000 in blocking buffer (1% [v/v] Triton X-100 and 10% [v/v] normal sheep serum in PBS). Alkaline phosphatase activity was detected in tissues by colorimetric assay using nitroblue tetrazolium (NBT)/5-bromo-4-chloro-3-indolyl-phosphate (BCIP) followed by mounting with Vectashield media containing 4′,6′-diamidino-2-phenylindole (DAPI; Vector Laboratories). When desired, microtubules were colocalized with the in situ signal using an anti-α-tubulin antibody conjugated to fluorescein isothiocyanate (FITC; 1:50 dilution; Sigma, St. Louis, MO). Controls in these experiments included hybridization in the absence of probe and hybridization with sense-strand RNA probe.

A multiple-tissue Northern blot (Clontech) was used to identify KRP3 transcripts in different rat tissues using the three KRP3 DNA fragments described above as probe (KRP3head, 72.1tail, and 85.2tail). Two different blot preparations were used for these experiments and gave identical results. The motor probe was labeled by mixed primer labeling using the kit from Boehringer Mannheim and [α^{32}P]dATP. Blots were hybridized to probe in ExpressHyb solution (Clontech) for 1 h at 68°C. After hybridization, blots were washed at high stringency and exposed to a Molecular Dynamics PhosphorImager screen (Amersham Pharmacia Biotech, Piscataway, NJ) for 3 days (KRP3head), 7 days (KRP3A, 72.5tail), or 5 days (KRP3B, 85.2tail).

Cell Purification

Spermatogenic cells were isolated as described previously [17] except that perfusion of the testicular arteries was omitted. Cells were released from the epithelium by sequential digestion with 0.5 mg/ml of collagenase and 0.5 mg/ml of trypsin and mechanical disruption. The resultant cell suspension was further purified by sedimentation at unit gravity (Staput method) through a 2–4% BSA gradient. Late pachytene spermatocytes and round spermatids were obtained from adult animals, whereas spermatogonia were obtained from 8-day-old animals. Sertoli cells were isolated from the rat (strain CD; Harlan Laboratory, Indianapolis, IN) as described previously [18]. Immature Sertoli cells were obtained from animals 17 days of age, whereas adult Sertoli cells were obtained from animals older than 70 days postpartum. After dissociation from the tubules, the cells were cultured in Dulbecco modified Eagle medium/F-12 containing 5% FBS and antibiotics at a cell density of approximately 2×10^6 per 35-mm dish. After 2 days of incubation at 33°C, the medium was replaced with fresh medium. Thereafter, the medium was changed every 2 days for 6 days. Contaminating germ cells were lysed with hypotonic solution on Day 3 as described previously [19]. Leydig cell contamination was measured histochemically by assessing 3-β-steroid dehydrogenase, and after 6 days, the culture was greater than 95% Sertoli cells.

Western Blot Analysis

Protein extracts were prepared from purified cell types and whole testis using a modification of published protocols [17, 20]. Briefly, decapsulated testes from adult or prepuberal rats or frozen pellets of purified gametogenic cells or Sertoli cells were homogenized in buffer containing protease inhibitors and centrifuged two times to remove cellular debris. For some experiments, enriched fractions of microtubule-associated proteins were prepared from crude lysates by microtubule affinity as described previously [21]. In this case, endogenous microtubules were supplemented with 250 μM bovine brain tubulin (Cytoskeleton, Denver, CO) stabilized with 10 μM paclitaxel in the presence of 1 mM GTP and 1 mM AMP-PNP (Sigma) at 37°C for 15 min followed by a 10-min incubation on ice. Kinesin-related proteins bind reversibly to microtubules in the presence of AMP-PNP, therefore providing a method for enrichment. Microtubules and associated proteins were pelleted by centrifugation through a 25% (w/v) sucrose cushion at 100 000 × *g* for 20 min at room temperature and resuspended in sample buffer for analysis.

Proteins were separated by PAGE through 10% (w/v) acrylamide gels, equilibrated in and electrophoretically transferred from the gel matrix to polyvinylidene fluoride membrane (BioRad Laboratories, Hercules, CA) in Towbin transfer buffer [22]. Proteins were detected on the membrane with the following primary antibodies: 1) KRP3head monoclonal antibody raised to the peptide HQATTEEEALNL present in both KRP3A and KRP3B coding sequences (gift of S. Brady, UT Southwestern Medical Center, Dallas, TX), 2) anti-KRP3Atail affinity-purified polyclonal antibody raised in rabbits against the unique peptide KLLNDKKTLENTD found in the tail domain of KRP3A, and 3) anti-KRP3Btail affinity-purified polyclonal antibody raised in rabbits against the unique peptide VSSGLSHVLPRSN found in the tail domain of KRP3B. Both peptides were synthesized by the Protein Sequence Core Facility, University of North Carolina at Chapel Hill, and were linked to keyhole limpet hemocyanin for antibody production or to an agarose support for affinity purification using the Sulfolink kit (Pierce, Rockford, IL). Immune complexes bound to the membrane were detected with a horse radish peroxidase-conjugated donkey secondary antibody diluted 1:1000 in TBST (20 mM Tris [pH 7.5], 154 mM NaCl, 2 mM EGTA, 2 mM $MgCl_2$, and 0.1% [v/v] Triton X-100; Jackson ImmunoResearch, Inc., West Grove, PA) and developed with enhanced chemiluminescence reagents from Amersham Pharmacia Biotech as described by the manufacturer.

Immunofluorescence

The KRP3 isoforms were detected in tissue sections essentially as previously described for isolated cells [4]. Testes were obtained from prepuberal or sexually mature rats (7, 14, 20, or 30 days or 8–10 wk; Sprague-Dawley; Harlan) and processed as described above for ISH except for an additional acetone rinse after sectioning. The tissue was blocked in 2% (w/v) BSA in TBST and incubated sequentially with primary and secondary antibodies.

Testis sections were incubated with affinity-purified KRP3Atail or unpurified KRP3Btail (the KRP3Btail polyclonal antibody was unstable after purification) isoform-specific polyclonal antibodies at 1:50 to 1:100 dilution in immunofluorescence blocking buffer (2% BSA and 0.1% azide in TBST) for 1 h, then rinsed three times in TBST. The KRP3head monoclonal antibody routinely gave much lower signal on tissue sections compared to that on Western blots and, therefore, was not used for immunofluorescence. The primary antibody was detected with donkey anti-rabbit immunoglobulin G conjugated to Texas Red (1:200 dilution; Jackson ImmunoResearch Laboratories) and nuclei stained with DAPI contained in the mounting media (Vectashield) or with Sytox green (Molecular Probes, Eugene, OR). The intracellular localization of KRP3-related anti-

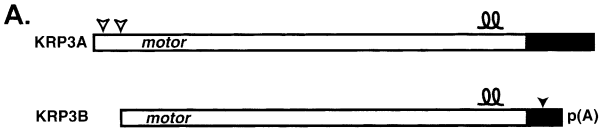

B.
MTRIQRFVGFFVFSGLDSERSRVSTESPPVMVKQTIQIFA
RVKPSVRKQQQGIYSIDEDEKLASSLEIVLPRDLADGFVN
NKRESYKFKFQRIFDQEAKQEIIFEIIAKPVAESTLAGYN
GTIFAYGQTGSGKTFTITGGAERYSDRGIIPRTLSYIFEQ
LQKDSSKIYTTHISYLEIYNECGYDLLDPRHEASKLEDLP
KVTILEDPDQNIHLKNLSLHQATTEEEALNLLFLGDTNRM
IAETPMNQASTRSHCIFTVHLSSKEPGSATVRHAKLHLVD
LAGSERVSKTGVGGLLLTEAKYINLSLHYLEQVIIALSEK
HRTHIPYRNSMMTSVLRDSLGGNCMTTMIATLSLEKRNID
ESISTCRFAQRVALIKNEAILNEEIDPRLMIVRLQKEIAD
LKAELAMVTGEQRTEALTEAELLQLEKLIASFVEDQDPES
RLEVGADLRKIHYCFHHFKKLLNDKKPLENTDLSESTTQQ
ACQEPVKDEEYTKLRSLLKQRDNEINELVNMLKKKK

C.
KQTIQIFARVKPSVRKQQQGIYSIDEDEKLASSLEIVLPRD
LADGFVNNKRESYKFKFQRIFDQEAKQEIIFEIIAKPVAES
TLAGYNGTIFAYGQTGSGKTFTITGGAERYSDRGIIPRTLS
YIFEQLQKDSSKIYTTHISYLEIYNECGYDLLDPRHEASKL
EDLPKVTILEDPDQNIHLKNLSLHQATTEEEALNLLFLGDT
NRMIAETPMNQASTRSHCIFTVHLSSKEPGSATVRHAKLHL
VDLAGSERVSKTGVGGLLLTEAKYINLSLHYLEQVIIALSE
KHRTHIPYRNSMMTSVLRDSLGGNCMTTMIATLSLEKRNID
ESISTCRFAQRVALIKNEAILNEEIDPRLMIVRLQKEIADL
KAELAMVTGEQRTEALTEAELLQLEKLIASFVEDQDPESRI
EVGADLRKIHYCFHHFKVNFNVSSGLSHVLPRSNCNKNSSC

FIG. 1. Schematic and predicted polypeptide sequence of KRP3 cDNA clones. **A**) KRP3A and KRP3B are identical in the area shown by the white boxes and divergent in that represented by the filled boxes. Two white arrowheads indicate the possible start sites of translation in KRP3A, whereas the filled arrowhead indicates the stop codons in the KRP3B cDNA. The poly(A) tail present in the KRP3B clone is shown. The motor domain of these proteins is located at the amino terminus, as indicated, and the region in each polypeptide that is predicted to form a coiled-coil structure is denoted with a coil above the schematic [14]. **B** and **C**) Predicted amino acid sequence for KRP3A and KRP3B, respectively, with the downstream start site in KRP3A indicated by a white arrowhead. The divergent sequence of each polypeptide is shaded. Homology to the signature 2 consensus of RCC1 is indicated in the KRP3B sequence by a solid underline (**C**), whereas homology to zinc finger DNA-binding proteins is shown with a dashed underline. The KRP3A and KRP3B sequences are available from GenBank/EMBL/DDJB under accession numbers AY035402 and AY035403.

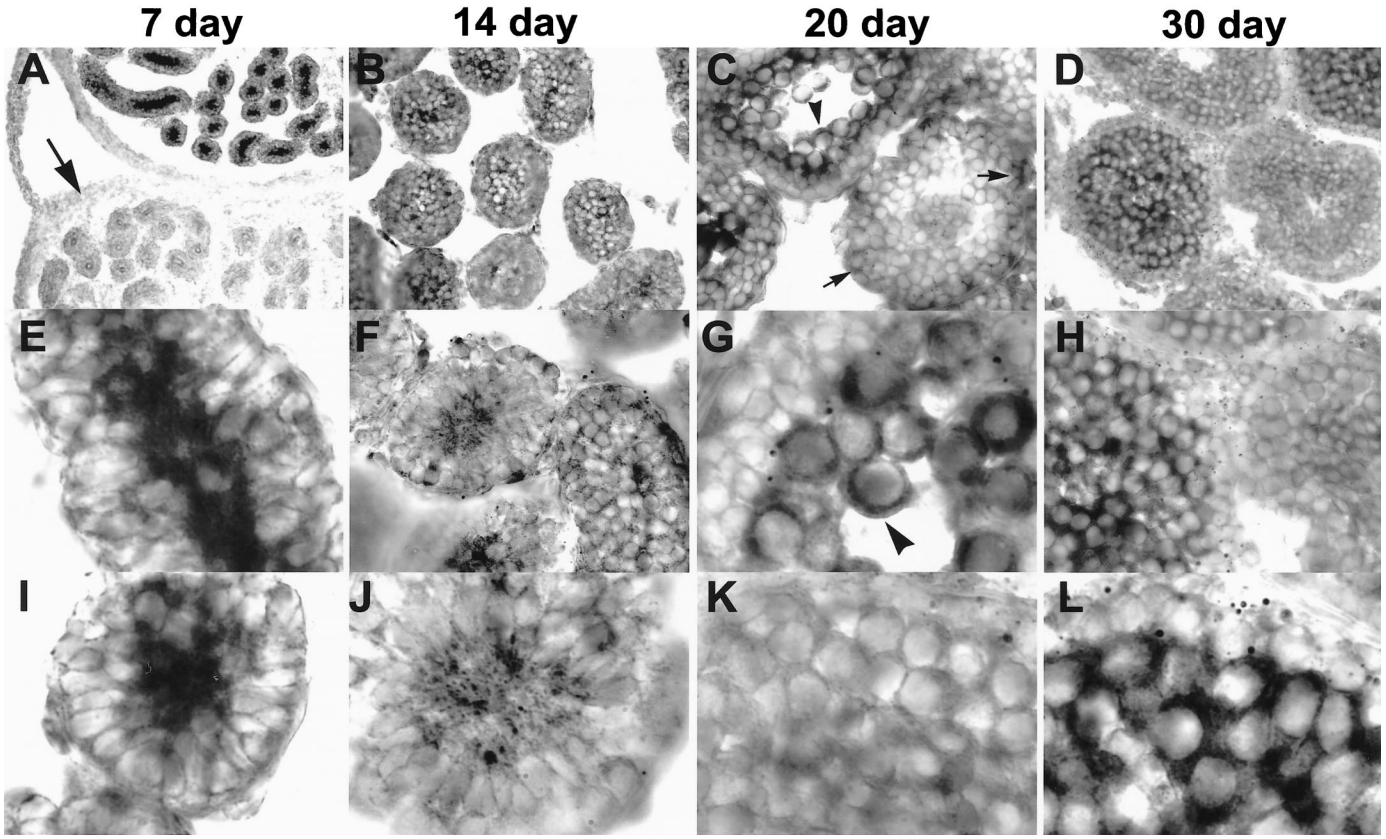

FIG. 2. Developmental expression of KRP3 mRNAs. The KRP3 mRNA was detected by ISH of Day 7, 14, 20, and 30 rat testis and epididymis (arrow, Day 7) using a probe to the KRP3head domain. Intense staining of pachytene spermatocytes is indicated by arrowheads (**C** and **G**). Staining of more basally located cells is indicated by arrows (**C**). The lower two photographs in each age group are a higher magnification of the same experiment. Magnification ×50 (**A–D**), ×100 (**G** and **H**), and ×250 (**E**, **F**, and **I–L**).

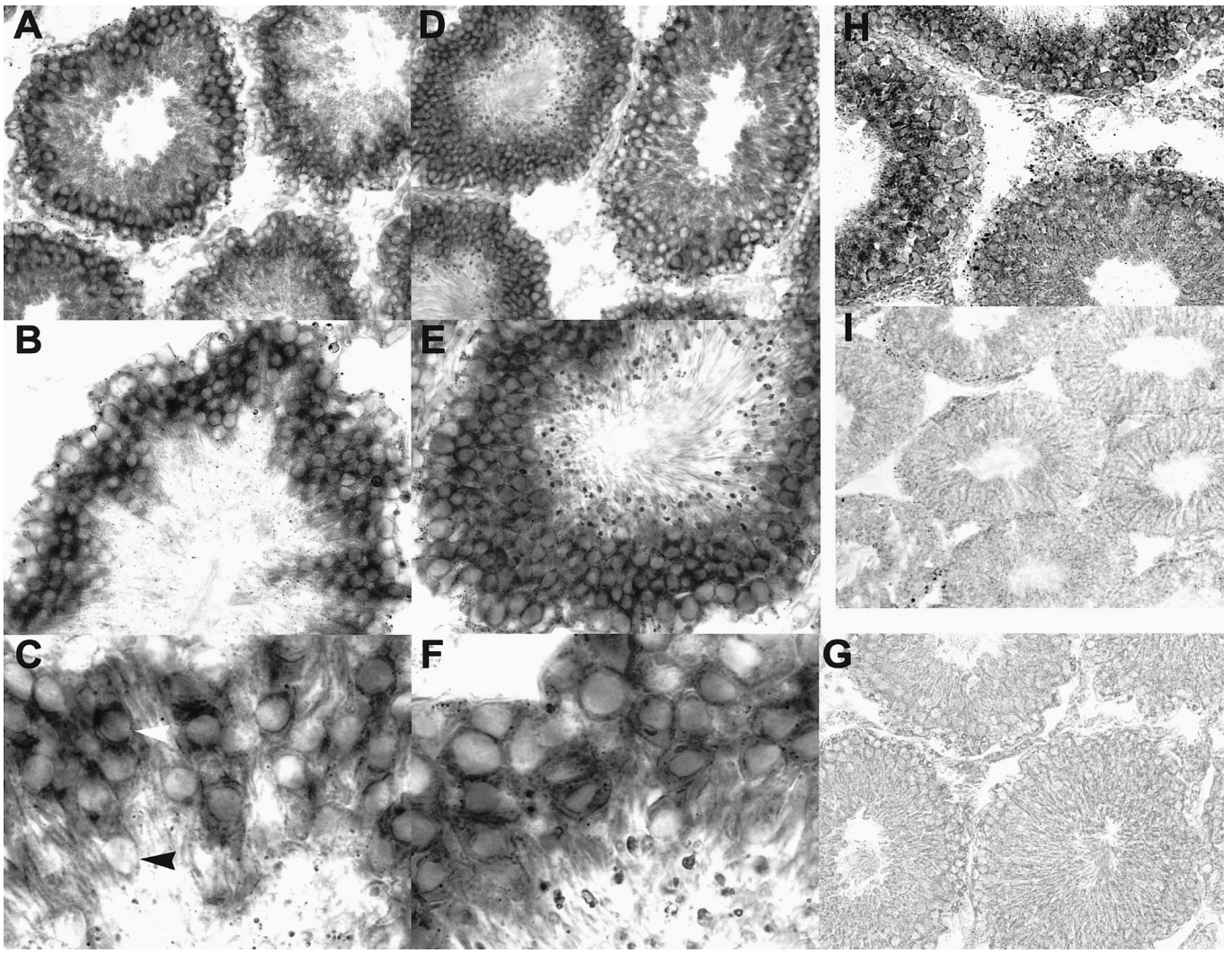

FIG. 3. ISH analysis of motor messages in normal adult testis. Motor messages were detected using antisense RNA probes labeled with DIG as described in *Materials and Methods.* Hybridization signals of KRP3head probe (**A–F**) and KRP2head probe (**H**) on testis sections developed with NBT/BCIP and visualized by bright-field illumination are shown. Hybridization with the sense probes for the respective messages are also shown (**G** and **I**). Magnification ×50 (**A**, **B**, and **G–I**), ×100 (**B** and **E**), and ×250 (**C** and **F**).

gens was observed with a Nikon E600 fluorescence microscope (Melville, NY) fit with appropriate filters and images captured with an Orca II CCD camera from Hamamatsu (Bridgewater, NJ) and analyzed with Metaview image analysis and acquisition software from Universal Imaging Corporation (Downingtown, PA). Controls for these experiments included a nonspecific antibody (anti-HIS6 monoclonal; Qiagen, Valencia, CA), omission of primary antibody, normal rabbit sera, and preincubation of primary antibody with the peptide antigen. Antibodies specific for Ran (rabbit anti-human Ran; Covance, Inc., Princeton, NJ) [23] and RCC1 (rabbit anti-*Xenopus* RCC1; gift of Dr. Yixian Zheng, Carnegie Institution of Washington, Baltimore, MD) were used to localize these proteins in testis sections. In some cases, samples were viewed with a Zeiss laser-scanning confocal microscope (LSM 510 Axiovert 200M; Carl Zeiss, Inc., Thornwood, NY) equipped with a 488/568/647-nm krypton-argon laser to allow simultaneous visualization of FITC and Texas Red. The individual optical sections were merged to produce one image and exported to Photoshop 6.0 (Adobe Systems Incorporated, San Jose, CA), with which the image was manipulated without alteration of data integrity.

RESULTS

Cloning of Two KRP3 Motor Isoforms in the Testis

Six kinesin-related cDNA fragments were identified previously in the rat testis [6]. Three of these demonstrated high sequence homology to motors involved in cell division, whereas the remaining three appeared to be unique. A cDNA fragment containing the head domain for one of the unique motors, KRP3, was used as probe to isolate cDNA clones from a rat testis cDNA library. Sequence analysis revealed two distinct species that were almost identical except for the sequence of their 3′ ends. The two unique clones were named KRP3A and KRP3B (Fig. 1A). Although the KRP3A clone contains a presumptive poly(A) tail, no stop codon was detected to terminate the long open-reading frame of 516 amino acids (predicted molecular weight, 58.7 kDa), suggesting that this clone may be incomplete. In addition, the KRP3A clone contains an alternative start site, being found 30 amino acids downstream (predicted molecular weight, 55.2 kDa; Fig. 1B, arrowhead). Neither site contains a match to the Kozak sequence [24]. The KRP3B clone contains an open-reading frame of 452 amino acids (predicted molecular weight, 51 kDa), with the KRP3B clone beginning immediately after the second presumptive start codon in KRP3A (Fig. 1A, open arrowhead). Each encodes an amino-terminal kinesin motor domain identical at the amino acid level. One nucleotide difference was detected in addition to the divergent tail domains and was located in the head domain.

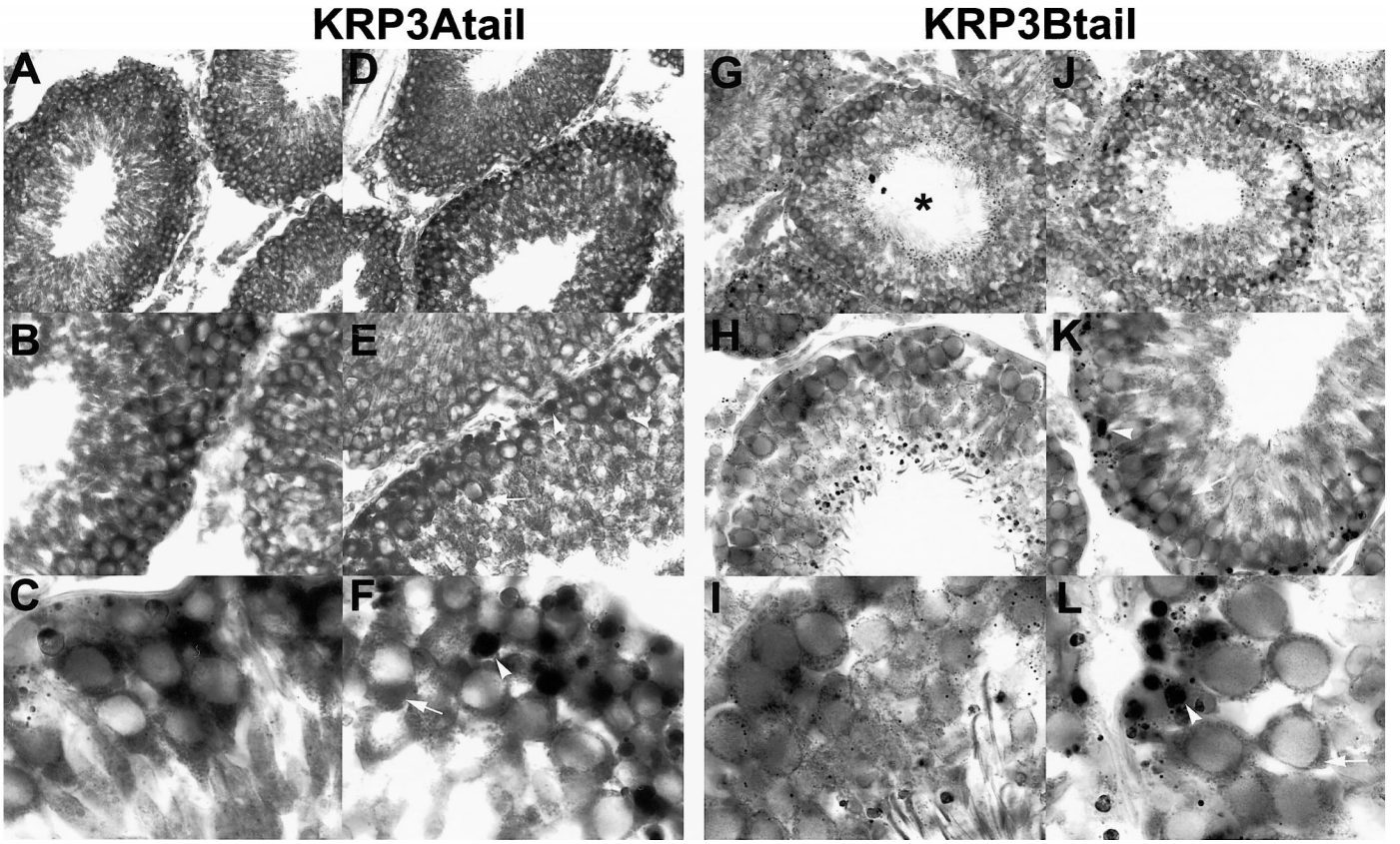

FIG. 4. ISH analysis of KRP3A and KRP3B messages. The KRP3 messages were detected using DIG-labeled antisense RNA probes to the tail fragments of KRP3A and KRP3B as described in *Materials and Methods*. Hybridization signal of KRP3Atail probe (**A–F**) and KRP3Btail probe (**G–L**) on testis sections developed with NBT/BCIP and visualized by bright-field illumination are shown. Arrowheads (**E**, **F**, **K**, and **L**) indicate the location of granular staining, and arrows show cells with more homogeneous staining. The asterisk indicates a tube cross-section of approximately stage V. Magnification ×50 (**A**, **D**, **G**, **J**), ×100 (**B**, **E**, **H**, **K**), and ×250 (**C**, **F**, **I**, **L**).

Neither protein shows high sequence homology, throughout its sequence, to known proteins entered into sequence databases. As expected, the highest level of homology is with the head domain of kinesin-related proteins. The most significant identity is with KIF6, a partial clone identified in mouse hippocampal cDNA [25]. The KRP3A/KRP3Bhead domains are approximately 95% identical to the KIF6head domain fragment. Although identified initially in the brain, KIF6 is expressed predominately in the testis [25].

Predicted Features of the KRP3A and KRP3B Polypeptides

To determine whether KRP3A and KRP3B contain a coiled-coil ''stalk'' domain typical of most kinesins, we examined their sequence with several secondary-structure prediction programs. Both KRP3A and KRP3B polypeptides contain a region with a small probability of forming a coiled-coiled structure [14]. The predicted coiled-coil region of these proteins is very short, however, and restricted to an approximately 50-amino-acid section located approximately 50 residues from the carboxyl terminus. In fact, using the more stringent prediction method of Berger et al. [15] the KRP3 polypeptides may not form coiled-coils (data not shown). The divergent amino acids are highlighted in the polypeptide sequences shown in Figure 1, B and C. Both tails are quite basic, each with an isoelectric point of almost nine.

The predicted protein sequences of both KRP3A and KRP3Btail domains were compared against the PROSITE database [26] to detect structural motifs and to the SCOP (structural classification of proteins) database [27] to detect any relationship with characterized protein families. In addition to matches to the *N*-glycosylation and casein kinase II phosphorylation sites, KRP3B contains an 82% match to the RCC1 signature 2 sequence [28]. Search of the SCOP database also revealed homology with the C2H2 class of zinc finger DNA-binding proteins (Fig. 1C, dashed underline). The KRP3Atail sequence did not display any significant homology to known protein motifs other than the casein kinase II phosphorylation consensus.

KRP3 Message Is Developmentally Expressed

Spermatogenesis is a developmental program initiated at the time of birth with the proliferation of spermatogonia. As the animal matures, progressively more differentiated cell types populate the seminiferous tubules. For example, 7 days after birth in the rat, the epithelium contains only spermatogonia and Sertoli cells, with meiosis beginning at approximately 14 days postpartum. Spermatids appear at approximately Day 20, and the full compliment of developing cell types is present by sexual maturity after Day 30. The expression pattern of KRP3 was surveyed during sexual development to determine whether specific cell types express this message in a developmentally regulated manner. Testes from prepuberal and puberal rats (7, 14, 20, and 30 days postpartum) were used for localization of KRP3

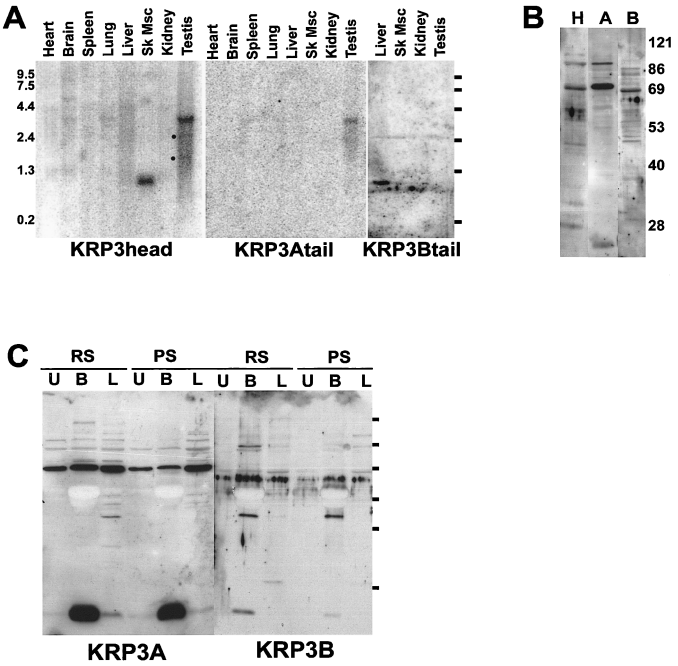

FIG. 5. Analysis of KRP3 isoform mRNA and protein distribution. The KRP3 transcripts were detected on a multiple-tissue Northern blot (**A**) with a probe to the KRP3head domain (left), the tail domain of KRP3A (center), and the tail domain of KRP3B (right). The KRP3A and KRP3B proteins were detected in testis extracts (**B**) using the KRP3head monoclonal (lane H) and antipeptide antibodies (lane A: KRP3tail; lane B: KRP3Btail) as described in *Materials and Methods.* Protein extracts were prepared from purified germ cells (**C**), including round spermatids (RS) and pachytene spermatocytes (PS) and kinesin-related molecular motors enriched by their affinity for microtubules as described in *Materials and Methods.* The supernatant from microtubule binding (unbound [U]), the microtubule pellet containing bound motors (B), and the high-speed supernatant from cell lysate (L) were separated by PAGE and blotted with the indicated antibodies. The marks in **C** indicate the positions of the molecular weight markers also used in **B**.

message by ISH using a probe to the head domain of this motor.

The KRP3 message is abundant in tubules from 7-day-old animals (Fig. 2, A, E, and I) and is considerably more abundant in the developing testis than in the epididymis (Fig. 2A). As cellular content becomes more complex at later time points, the KRP3 signal is associated with cells located more toward the center of developing tubules (Fig. 2, C and G, arrowheads), with some signal at the basal aspect in Day 20 tubules (Fig. 2C, arrows). During this developmental series, KRP3 staining decreases in Day 15 animals (Fig. 2, B, F, and J), followed by staining of increasingly numerous cells so that by Day 30, when spermatocytes are rapidly dividing, KRP3 signal is again prominent and clearly stage specific (e.g., Fig. 2, D and H). Two patterns of staining are shown for Day 20 and Day 30 testes: dark staining of cells interior to the tubule (Fig. 2G) that expand to fill the tubule at 30 days (Fig. 2H), and lighter staining of adjacent tubules (compare tubules in the left and right sides of Fig. 2H). This developmental pattern of expression is consistent with the localization of KRP3 message in pachytene spermatocytes in adult testis (Fig. 3); however, basal staining at earlier times suggests expression in Sertoli cells or earlier germ cells.

KRP3 Messages Are Expressed in Cells of the Seminiferous Epithelium

To identify the testicular cell types that express KRP3, we performed ISH using the head domain probe on testis sections from adult rat. The KRP3 message is present in many stages; however, the pattern of expression clearly changes as a function of the spermatogenic cycle (Fig. 3, A and B). The KRP3 message staining is striking in cycle stage X and easy to describe (Fig. 3C). At this stage, KRP3 is not strongly expressed until pachytene of the first meiotic prophase (Fig. 3C, white arrowhead), and expression appears to decline in condensing spermatids (Fig. 3C, black arrowhead). The KRP3 staining is also abundant in other stages, including stage IV (Fig. 3, D–F), in which round spermatids are stained. To determine whether the unique localization of KRP3 mRNA is specific to KRP3 or common to other motor protein messages, an antisense probe to the previously characterized KRP2 molecular motor was used for hybridization. The KRP2 message is expressed in a stage-specific manner and is localized to the adluminal compartment in positive tubule sections (Fig. 3H) [6]. This distribution is unlike that of the KRP3 motor, which is found more basally in the epithelium.

Gene Expression of KRP3A and KRP3B

To investigate the expression pattern of the two KRP3 isoforms in the testis, ISH was conducted using the unique tail domains of KRP3A and KRP3B as probe. Digoxigenin-labeled RNA probes gave similar patterns for both KRP3A and KRP3B (Fig. 4, left and right set of panels, respectively). For both probes, the hybridization signal was localized to the basal region of the epithelium in a pattern similar, but not identical, to that seen for the KRP3head domain probe and appeared to be less abundant (Fig. 4, A, D, G, and J). However, close examination reveals that these messages are found in cells slightly earlier in the developmental pathway than those detected with the KRP3head domain (Fig. 4, B, E, H, K, and higher magnification in the bottom panels). Furthermore, a granular signal was present in discrete regions in a small subset of tubules in which early spermatids were present (stages IX and X in the rat) (Fig. 4, E, F, K, and L, arrowheads). No such granular signal was detected in any samples stained with the KRP3head domain probe. Negative controls including no probe, antisense probe, or no primary antibody showed no hybridization (data not shown).

All three KRP3 probes showed more diffuse cellular staining in cells in the basal region of the epithelia. These positive tubules (e.g., Fig. 4G, asterisk) between stages IV and VI displayed staining of basal cells and lacked the granular appearance of the hybridization signal found in stage IX and X tubules.

KRP3 Motors Are Encoded by Multiple Transcripts

Our analysis of the expression pattern of the KRP3 motors indicates that they are present in multiple cell types in the seminiferous epithelium. To determine whether this heterogeneity reflects a diversity of KRP3 transcripts, we con-

FIG. 6. Immunofluorescent localization of KRP3 proteins in adult rat testis. The KRP3Atail (**A–F**) and KRP3Btail (**G–L**) antibodies were reacted with fixed, frozen sections of normal adult rat testis and detected with a Texas Red-conjugated secondary antibody, whereas DNA was detected with Sytox green). Polar staining of the nucleus in round spermatids is visible (**B**, **H**, **M**, and **N**, arrows); staining of the head of elongating spermatids is also visible (**E** and **K**). Normal rabbit serum was used as a negative control (**O**). Magnification ×50 (**A–C** and **G–H**), ×100 (**D–F** and **J–L**), and ×250 (confocal images in **M** [KRP3A] and **N** [KRP3B]).

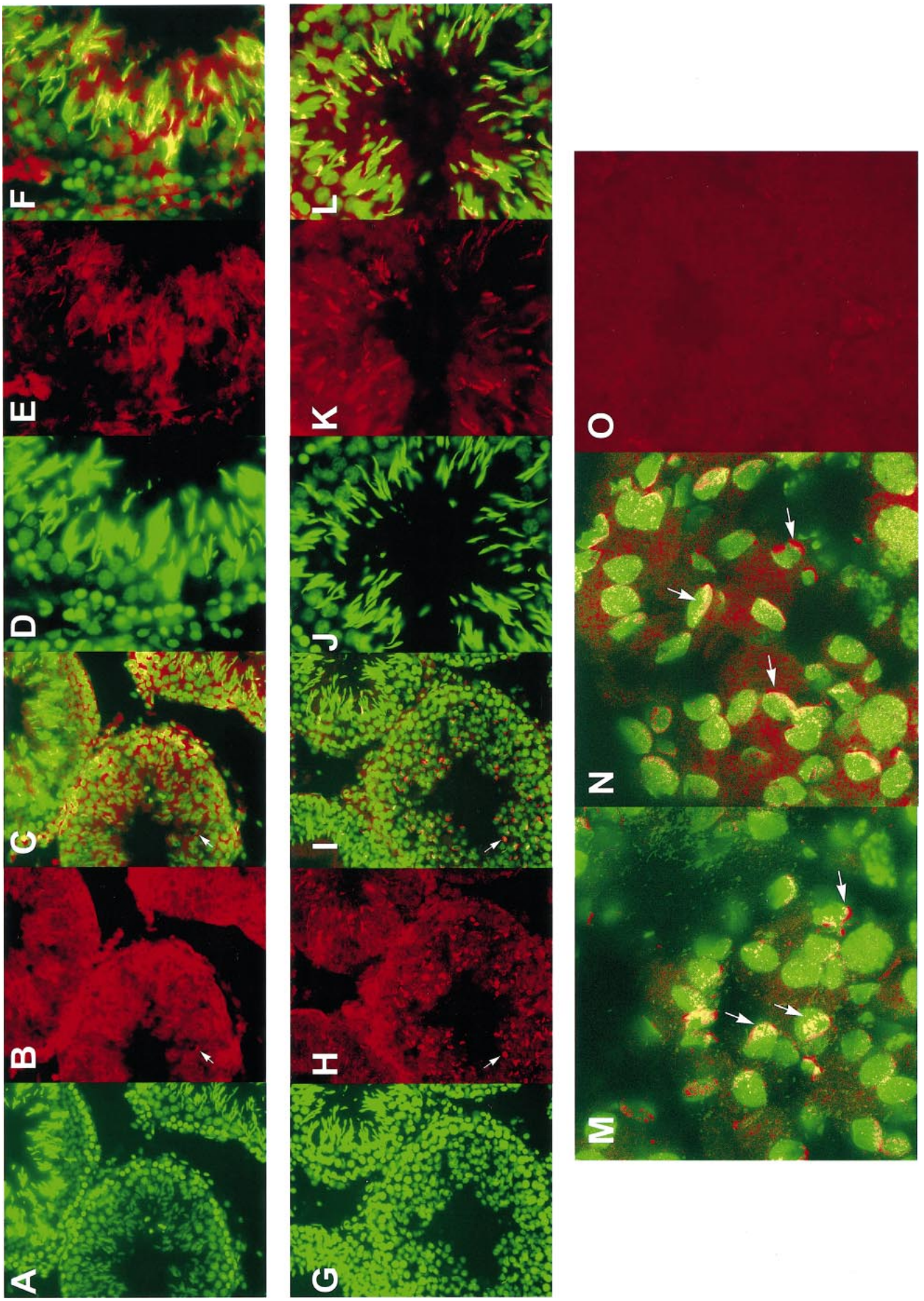
A
B
C
D
E
F
G
H
I
J
K
L
M
N
O

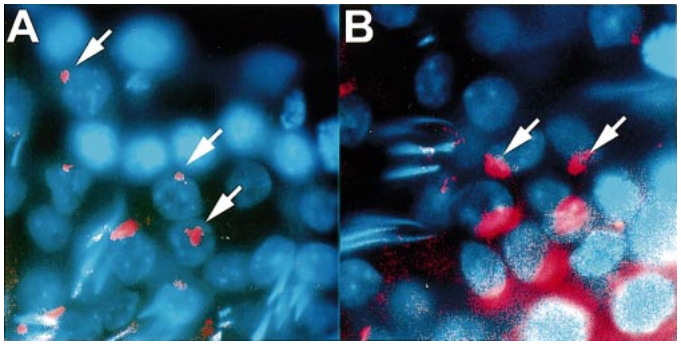

FIG. 7. KRP3B staining of early spermatids. The KRP3B tail antibody was used to stain fixed, frozen sections of rat testis and was detected with a Texas Red-conjugated secondary antibody and stained for DNA with DAPI. Sections were viewed using a triple-pass filter to visualize KRP3B with respect to the nucleus. Arrows indicate staining outside the spermatid nucleus in a polar fashion. Two views are shown (**A** and **B**).

ducted Northern blot analysis of mRNA obtained from multiple tissues using the probes previously used for ISH. As expected, the KRP3head probe, which detects all isoforms, recognizes at least three species in testicular mRNA: a relatively abundant transcript of 3.2 kilobases (kb), and two less abundant transcripts of 2.7 and 1.7 kb (Fig. 5A, dots beside lane). This finding is consistent with our previously published results concerning the sizes of KRP3 messages [6]. The 3.2-kb band is most intense in the testis sample but is also visible in lung and brain (Fig. 5A; data not shown). Strikingly, a small transcript was detected in skeletal muscle at approximately 750 nucleotides and was also visible in other experiments. The size of this transcript is quite unusual given that a typical motor domain alone would be encoded by an approximately 1-kb message.

The KRP3Atail probe detected messages that were much less abundant than those detected by the KRP3head probe (Fig. 5A, center panel); a 3.2-kb transcript was detected in testis. This finding suggests that the 3.2-kb transcript detected with the KRP3head probe might contain the KRP3Atail sequence. However, the low abundance of the KRP3Atail transcript compared to that of the KRP3head-reactive species is consistent with KRP3Atail being a subset of KRP3 species of this size in the testis. A smaller KRP3Atail transcript of 2.7 kb was also visible in the testis (Fig. 5A, center panel). The KRP3Btail-positive transcripts were also not abundant (Fig. 5A, right panel). Transcripts of approximately 2.7 kb were detected in testis, spleen, and liver (Fig. 5C). In addition, an approximately 750-nucleotide species was found in the liver sample. Clearly, the KRP3 probes detect multiple isoforms, some of which may be tissue specific.

KRP3 Motors Are Comprised of Multiple, Related Isoforms

To determine the precise cell types and intracellular structures to which these motors associate, we developed immunological reagents to the KRP3 isoforms. A monoclonal antibody raised to a peptide found in the KRP3 head domain and common to the isoforms was used to identify KRP3-related proteins by immunoblot. The KRP3head antibody specifically recognizes a bacterially expressed KRP3 head domain fragment (S.T. Brady, personal communication). This antibody detects at least three polypeptides in testis lysates (Fig. 5B, lane H): proteins of approximately 100 kDa, and a doublet at 70 kDa. Interestingly, the KRP3Atail antibody recognizes multiple polypeptides in total testis lysate of 100 kDa, 70 kDa, and a small protein of approximately 22 kDa (Fig. 5B, lane A). The KRP3Btail antibody recognizes a protein of approximately 68 kDa (Fig. 5B, lane B). The proteins detected with each antibody overlap with those recognized by the KRP3head antibody. The KRP3Atail antibody detects three proteins identical in size to those found by the KRP3head antibody, and the KRP3Btail antibody recognizes an additional protein that is also apparently detected by the KRP3head antibody.

This complex pattern indicates significant heterogeneity in the KRP3 polypeptides and reflects the multiple transcripts seen by Northern blot analysis (Fig. 5A). Although the smallest transcript detected by Northern blot analysis was not visible in the testis sample, a 22-kDa protein consistent with translation from this transcript was detected in

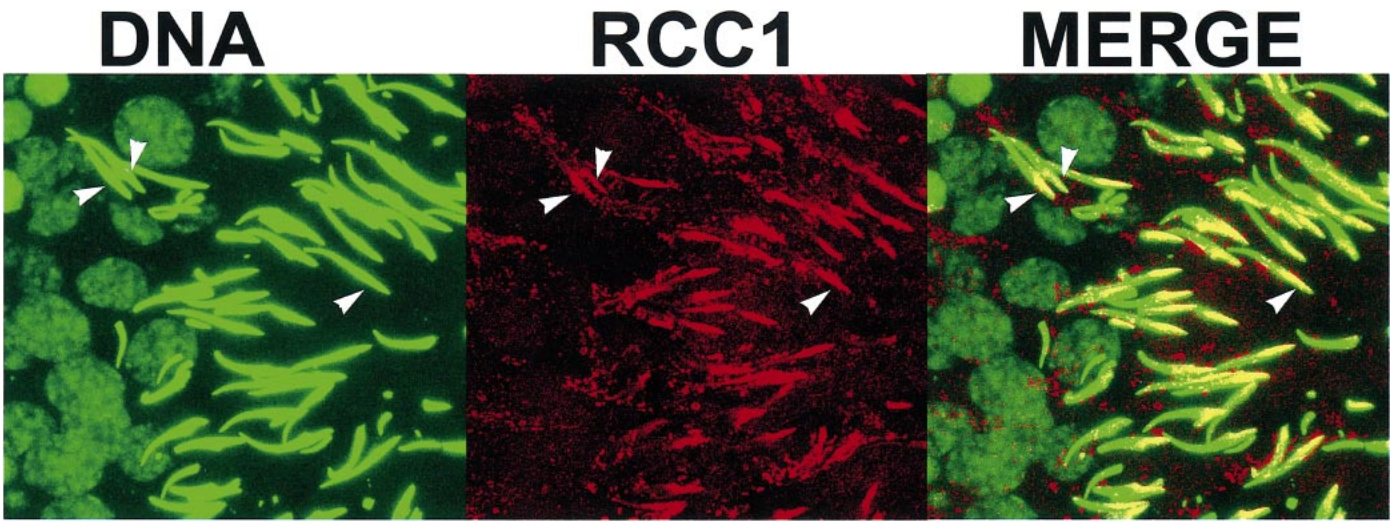

FIG. 8. RCC1 is localized to the caudal end of elongating spermatids. A polyclonal anti-RCC1 antibody raised against the *Xenopus* protein was used to localize this protein in the mammalian testis. In the leftmost panel, DNA is visualized by staining with Sytox green. The middle panel shows detection of RCC1 using a Texas Red-conjugated secondary antibody, whereas the rightmost panel is the merged green and red images. The arrowheads indicate colocalization of the RCC1 protein with the caudal region of the spermatid head. Magnification ×250.

total testis lysate and purified germ cells (Fig. 5C). In addition, the 2.7- and 1.7-kb transcripts found in testicular mRNA agree with the 100- and 70-kDa doublet detected by Western blot analysis of testis extract. Although a protein of approximately 116 kDa, predicted from the 3.2-kb transcript, was not strongly represented on immunoblot, in certain preparations we were able to detect higher-molecular-weight species with these antibodies (Fig. 5B, lane H).

KRP3A- and KRP3B-Related Polypeptides Are Expressed in Round Spermatids and Pachytene Spermatocytes

Molecular motor proteins were crudely purified from germ cell lysates by their affinity for microtubules in the presence of the nonhydrolyzable ATP analogue AMP-PNP and the fractions immunoblotted with the KRP3Atail and KRP3Btail antibodies (Fig. 5C). Both the 70- and the 22-kDa KRP3A-reactive polypeptides are found in spermatids and spermatocytes. The 68-kDa protein detected in whole-testis lysate with the KRP3B antibody is also found in spermatids and spermatocytes. In addition, a 48-kDa protein was detected in these cells; this size is consistent with translation from the 1.8-kb KRP3B clone. The enrichment of the 22-, 48-, and 68-kDa polypeptides in the microtubule-bound fraction (Fig. 5C, compare lanes labeled B with those labeled U) indicates the presence of a kinesin-like motor domain in these polypeptides. No polypeptides of approximately 70 kDa were detected in the total lysates or in the microtubule-bound fraction from adult Sertoli cells; however, the 22-kDa protein was detected in the bound fraction from these cells (data not shown).

KRP3A and KRP3B Are Associated with Developing Spermatids

Immunological reagents were developed to determine more accurately whether the KRP3 motors associate with specific intracellular structures in testicular cells by indirect immunofluorescence. The KRP3head monoclonal antibody proved to be unsuitable for indirect immunofluorescence and was not used in these studies. Isoform-specific antibodies were raised in rabbits against peptides unique to the tail domain of each isoform (see *Materials and Methods*). Immunolocalization using the KRP3A (Fig. 6, A–F) and KRP3B (Fig. 6, G–L) antipeptide antibodies showed a similar, but not an identical, pattern. Both antibodies stain the nucleus of round (Fig. 6, B and H, arrows) and elongate spermatids (Fig. 6, E and K), although staining with the anti-KRPA antibody displayed a generalized background. Higher magnification revealed that both KRP3A- and KRP3B-isoform antibodies stain a roughly C-shaped region at one pole of the nucleus in round spermatids, presumably the acrosome (Fig. 6, M and N, arrows).

In addition, KRP3B was detected in very early spermatids, being found on the surface of the nuclei in these cells (Fig. 7, A and B, arrows). In some cases, a fibular network was found to cover a small patch on the nuclear membrane (data not shown). Both antibodies also showed a granular basal staining in stage IX tubules similar to that seen by ISH (Fig. 4). Negative controls for these experiments included no primary antibody, incubation with normal rabbit sera (Fig. 6O), or preabsorption with the antigenic peptide (data not shown); all showed negligible signal compared to the experimental sample.

Ran and Its Guanine Exchange Factor, RCC1, Are Associated with the Nucleus of Developing Spermatids

The localization of KRP3 isoforms to the elongating sperm head suggested a possible role in sperm head restructuring and/or chromatin condensation. Based on the homology of KRP3B with RCC1, an antibody to RCC1 was used to localize this protein required for chromatin condensation to cells of the testis. In addition to generalized cellular staining, particularly in the cytoplasm of spermatogonia and spermatocytes, conspicuous staining was seen at the caudal end of the nucleus of elongating spermatids (Fig. 8, arrowheads). This staining was distinct from that of the KRP3-isoform antibodies and was located in a region of the approximately step-13 spermatid head occupied by the manchette structure rather than the homogeneous staining of the nucleus displayed by the KRP3 antibodies.

To determine whether the small GTPase Ran is associated with spermatids along with RCC1, its guanine exchange factor (GEF), and/or KRP3 motors, we localized Ran in adult testis sections. Ran is present in numerous cell types in the epithelium, being concentrated in the nuclei of pachytene spermatocytes (Fig. 9K, open arrows) and elongate spermatids (Fig. 9, B and C, arrowheads). The distribution of Ran in approximately step-13 spermatids is distinct from its GEF RCC1 (Fig. 8), being found throughout the spermatid head. In some individuals, a line of Ran staining is seen to outline the spermatid head (Fig. 9, B and C, arrows). In addition, Ran is localized to one pole of round spermatids (Fig. 9, E and F, arrows). Ran staining associated with spermatid nuclei is seen throughout spermiogenesis, including spermatids just before spermiation (Fig. 9, E and F, arrows). In many views, Ran staining appears to spread over one pole of the spermatid nucleus (Fig. 9, H and I, arrows) in a manner similar to that seen for KRP3 isoforms (Fig. 6H). In addition, Ran staining takes the form of a disc-shaped structure within the nucleus of a subset of spermatocytes (Fig. 9L, open arrows) in approximately stage II tubules before Ran becomes strongly apparent on round spermatids.

DISCUSSION

The process of spermatogenesis involves profound rearrangement of the microtubule cytoskeleton of germ cells with the formation and dissolution of several microtubule complexes, including the mitotic and meiotic spindles and the manchette. In addition to striking changes in the shape of male gametes during spermatogenesis, the shape and content of the spermatid nucleus changes dramatically as well. We have identified new kinesin-related molecular motors, KRP3 isoforms, that are associated with developing male germ cells and that may play roles in transformation of the spermatid nucleus.

Previously, KRP3 was shown to be expressed in cells of the rat seminiferous epithelium [6]. Initial library screening using the KRP3head domain identified earlier as probe revealed heterogeneity in KRP3 clones. At least two new kinesin-related cDNAs containing the KRP3head domain were identified in the rat testis. These clones, termed KRP3A and KRP3B, are identical to one another for most of their lengths, but they diverge 1287 nucleotides from the ATG start codon in KRP3A. Genetic mapping experiments suggest that a common gene encodes these two cDNAs. Probes specific for each tail domain cosegregate with one another and also with a head domain probe (N.A. Jenkins and N.G. Copeland, personal communication).

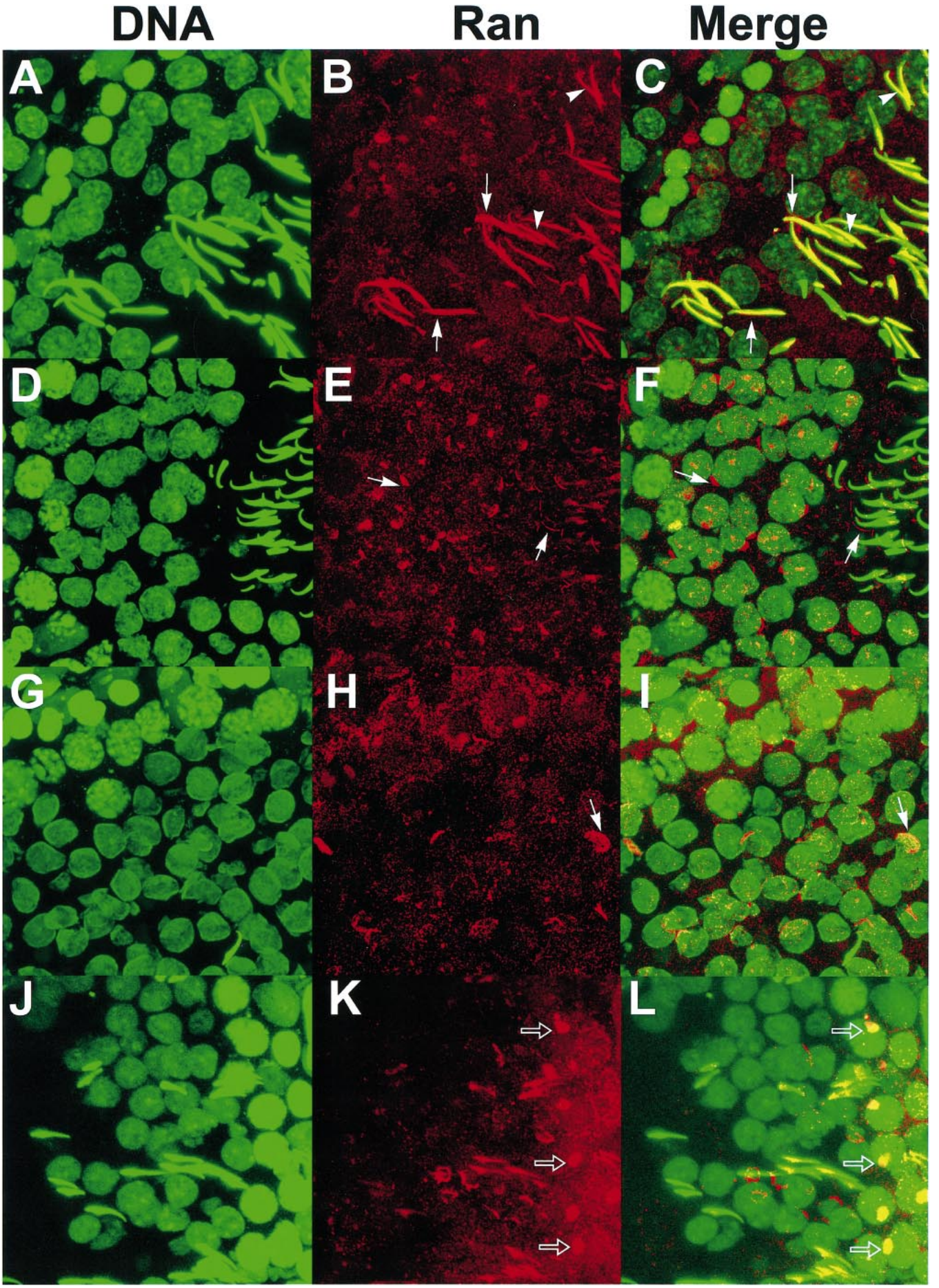
DNA
Ran
Merge
A
B
C
D
E
F
G
H
I
J
K
L

Although the KRP3A cDNA clone contains a presumptive polyadenylation site, no stop codon was detected, despite sequencing of multiple clones in both directions. This suggests that the KRP3A clone may be incomplete at its 3′ end. A very closely related human genomic clone was discovered during a database search that contains a peptide with 77% amino acid identity in the region of overlap with KRP3A [29]. This clone continues beyond the 3′ end of our KRP3A clone and contains a run of 13 A residues interrupted by 2 Gs to encode a lysine-rich peptide instead of the stretch of 14 consecutive A residues present in KRP3A. We predict, therefore, that the poly(A) tract at the 3′ end of the KRP3 clone is not added posttranscriptionally to form a poly(A) tail but, instead, encodes a string of lysine residues. If this is true, the predicted molecular weight of KRP3A could range between 65 and 68 kDa. This interpretation is supported by detection of KRP3A polypeptides at approximately the predicted size using Western blot analysis.

The KRP3head domain probe detected KRP3 message in pachytene spermatocytes in adult testis, but KRP3 message was also detectable in other cell types. That KRP3 messages are expressed in multiple cell types was further established by ISH of testis taken from prepuberal and puberal animals. The KRP3 message is strongly expressed in tubules from animals at 7 days postpartum, indicating expression in dividing spermatogonia and/or Sertoli cells. At 20 days postpartum, two distinct cell types are stained; basal cells, and proliferating spermatocytes in the interior of the tubule. In 30-day-old testis, the pattern of expression is clearly stage specific, with some tubules containing strongly stained cells whereas others are completely devoid of KRP3 expression.

The heterogeneity of the KRP3 cDNA clones and expression patterns is reflected in the various species detected by Northern and Western blot analyses. Three distinct transcripts were detected in the testis. Two of these, the 2.7- and the 1.7-kb transcripts, agree with 110- and 68- to 70-kDa polypeptides seen by Western blot analysis. A 116-kDa protein corresponding to translation from the 3.2-kb transcript is not seen consistently in our preparations, perhaps due to proteolysis or poor reactivity. In addition, a very small transcript of approximately 750 nucleotides was discovered in skeletal muscle. This size is sufficient to encode the 22-kDa protein found in several cell types and tissues, including the testis. The KRP3A and KRP3Btail probes detected much less abundant transcripts that appeared to comprise a subset of those detected by the conserved head probe. Neither of the clones we describe here is long enough to contain the 3.2-kb transcript detected with the head probe and the KRP3Atail probe.

Three prominent bands of 110 kDa and a doublet at 68–70 kDa were detected in testis lysate with the KRP3head antibody that recognizes an epitope conserved in this small family of motors. Analogous to the results of Northern blot analysis, multiple species were detected by Western blot analysis, with more proteins being reactive to the KRP3head antibody than to the tail antibodies, as expected. Each antitail antibody strongly recognized a unique subset of those polypeptides recognized by the KRP3head antibody. Our finding that the tail antibodies, particularly anti-KRP3Atail, recognize more that one polypeptide indicates that the recognized epitope is found on more than one protein. This supports the idea that generation of KRP3 isoforms is complex and probably involves alternative splicing.

Antibodies made to the predicted tail domains of KRP3A and KRP3B produced a very similar, but not identical, immunofluorescence pattern. Western blot analysis indicates that the tail antibodies recognize unique proteins, and their similar staining of the spermatid head suggests that this group of proteins may have a common function in germ cells generally and in spermatids specifically. Both antibodies stain the rim of the nucleus of round spermatids. However, KRP3A appears to be distributed more diffusely in the testis than KRP3B, perhaps reflecting the interaction of this antibody with multiple proteins, but both antibodies stain spermatids throughout the transformation of spermiogenesis. Indeed, early in development, KRP3B staining was seen adjacent to the nuclei of pachytene spermatocytes, forming a small patch on the surface of the spermatocyte nuclei. We also observed a granular staining in both ISH and immunofluorescent experiments using KRP3tail probes. In both cases, staining was found at the basal area of seminiferous tubules around the time of spermiation. These granules are morphologically similar to residual bodies and are present at a time when residual bodies are found at the base of the epithelium. Spermatid-associated KRP3 message and protein might be discarded in residual bodies on release of sperm into the lumen.

Perhaps the most intriguing finding of this work is the juxtaposition of Ran with KRP3 motors in round and elongating spermatids. Ran is a small GTPase whose role in nuclear transport has been well characterized. Recently, Ran has been shown to be essential in stabilizing microtubules during spindle formation along with its specific binding partners [30–32]. Our localization of Ran to the nucleus of developing spermatids places this regulatory protein at the ideal site to control the microtubule rearrangements and nuclear reorganization that occur during spermiogenesis. Indeed, the localization of RCC1 to the spermatid manchette implicates this GEF, along with Ran, in the assembly and function of the numerous microtubules that comprise the manchette, a structure that is thought to function in nuclear shaping and cytoplasmic redistribution during spermiogenesis [33–35]. The localization of a signaling molecule to the spermatid manchette has precedent; previously, a testis-specific serine/threonine protein kinase was found to be localized to this interesting structure [36].

We propose that Ran may also be involved in the restructuring and/or motility of the spermatid nucleus, possibly involving KRP3 motors. Very early in spermiogenesis, the spermatid nucleus becomes visibly polarized, with the formation of the acrosome at one pole. The nucleus then moves to the cell membrane, imparting this polarity on the cell itself and defining the polarity of the terminal cell, the spermatozoon. During this time, both Ran and KRP3 motors are found to be associated with the nucleus of round spermatids in a polarized fashion. Ran might be localized at a specific site within the nucleus to organize the polarized formation of membrane components and microtubule

FIG. 9. Ran is localized to the nuclei of spermatids and spermatocytes. A polyclonal antibody to human Ran was used to localize this small GTPase to fixed, frozen sections of rat testis. The Ran antibody was detected with a Texas Red-conjugated secondary antibody (middle panels), and the DNA was stained with Sytox green (left panels). Arrowheads indicate staining of elongate spermatid nuclei, whereas the arrows (**B**, **E**, and **H**) indicate staining associated with spermatid nuclei at different developmental stages. Open arrows (**K** and **L**) denote Ran staining of spermatocytes. Magnification ×250.

structures for spermatid development. This idea is supported by the detection of Ran in the nucleus of spermatocytes to form a disc-shaped structure at one pole of the nucleus (Fig. 9L).

Certain views of spermatids reactive for Ran and KRP3 isoforms show staining in a shape similar to that of the developing acrosome, including an acrosomal granule. Nuclear reshaping and formation of the acrosome occur in coordination during spermiogenesis, and these events likely are regulated by a common mechanism. For example, a KRP3 isoform could be involved in transport of vesicles to form the acrosome at a site predetermined by the location of signaling molecules. Similarly, nucleation and stabilization of manchette microtubules in a directed manner on the spermatid nucleus could be accomplished through a common signaling mechanism. Acrosome formation is dependent on microtubules and shares features with vesicle transport in other systems [37, 38]. The KRP3B staining in early spermatids before formation of the acrosome is very similar to the placement and structure of the Golgi apparatus in these cells. Indeed, the staining we observe for KRP3 motors in round spermatids is almost identical to the localization of Golgi and perinuclear theca markers to the developing bull acrosome [39].

Another possible function of KRP3 motors, consistent with their immunolocalization to spermatid heads and expression by Sertoli cells, is in microtubule-based movement of elongating spermatids within the epithelium [10, 40]. Recently, an isoform of cytoplasmic dynein was localized to the apical crypts concentrated in areas juxtaposed to the sperm head and postulated to be one motor responsible for translocation toward the apical aspect of the cell [5, 41]. However, a candidate plus-end-directed motor responsible for movement of spermatids toward the base of the epithelium has not been identified. The KRP3 isoforms are putative plus-end-directed motors associated with the spermatid head that might be involved in the basal translocation of spermatids. Individual isoforms might have other roles in spermatid maturation, including formation of the acrosome and/or spermatid head remodeling. The motor isoforms described here are excellent candidates for motors involved in the complex cellular transformations that occur during spermiogenesis and are likely targets for regulation during the dramatic changes in the spermatid nucleus.

ACKNOWLEDGMENTS

We thank Virginia Best, Mark Albertino, Colleen Nichols, Robin Wray, and Purnima Jani for providing expert technical assistance and Dr. Scott Brady for critical reading of the manuscript.

REFERENCES

1. Endow SA. Microtubule motors in spindle and chromosome motility. Eur J Biochem 1999; 262:12–18.
2. Hirokawa N. Kinesin and dynein superfamily proteins and the mechanism of organelle transport. Science 1998; 279:519–526.
3. Goodson HV, Valetti C, Kreis TE. Motors and membrane traffic. Curr Opin Cell Biol 1997; 9:18–28.
4. Navolanic PM, Sperry AO. Identification of isoforms of a mitotic motor in mammalian spermatogenesis. Biol Reprod 2000; 62:1360–1369.
5. Miller MG, Mulholland DJ, Vogl AW. Rat testis motor proteins associated with spermatid translocation (dynein) and spermatid flagella (kinesin-II). Biol Reprod 1999; 60:1047–1056.
6. Sperry AO, Zhao LP. Kinesin-related proteins in the mammalian testes: candidate motors for meiosis and morphogenesis. Mol Biol Cell 1996; 7:289–305.
7. Hall ES, Eveleth J, Jiang C, Redenbach DM, Boekelheide K. Distribution of the microtubule-dependent motors cytoplasmic dynein and kinesin in rat testis. Biol Reprod 1992; 46:817–828.
8. Molina I, Baars S, Brill JA, Hales KG, Fuller MT, Ripoll P. A chromatin-associated kinesin-related protein required for normal mitotic chromosome segregation in *Drosophila*. J Cell Biol 1997; 139:1361–1371.
9. Wang W, Chi T, Xue Y, Zhou S, Kuo A, Crabtree GR. Architectural DNA binding by a high-mobility-group/kinesin-like subunit in mammalian SWI/SNF-related complexes. Proc Natl Acad Sci U S A 1998; 95:492–498.
10. Beach SF, Vogl AW. Spermatid translocation in the rat seminiferous epithelium: coupling membrane trafficking machinery to a junction plaque. Biol Reprod 1999; 60:1036–1046.
11. Carazo-Salas RE, Guarguaglini G, Gruss OJ, Segref A, Karsenti E, Mattaj IW. Generation of GTP-bound Ran by RCC1 is required for chromatin-induced mitotic spindle formation. Nature 1999; 400:178–181.
12. Wilde A, Zheng Y. Stimulation of microtubule aster formation and spindle assembly by the small GTPase Ran. Science 1999; 284:1359–1362.
13. Hetzer M, Bilbao-Cortes D, Walther TC, Gruss OJ, Mattaj IW. GTP hydrolysis by Ran is required for nuclear envelope assembly. Mol Cell 2000; 5:1013–1024.
14. Lupas A, Van Dyke M, Stock J. Predicting coiled coils from protein sequences. Science 1991; 252:1162–1164.
15. Berger B, Wilson DB, Wolf E, Tonchev T, Milla M, Kim PS. Predicting coiled coils by use of pairwise residue correlations. Proc Natl Acad Sci U S A 1995; 92:8259–8263.
16. Komminoth P. Detection of mRNA in tissue sections using DIG-labeled RNA and oligonucleotide probs. In: Non-Radioactive In Situ Hybridization Application Manual. Mannheim, Germany: Boehringer Mannheim GmbH; 1996: 126–135.
17. Bellve AR, Cavicchia JC, Millette CF, O'Brien DA, Bhatnagar YM, Dym M. Spermatogenic cells of the prepuberal mouse. Isolation and morphological characterization. J Cell Biol 1977; 74:68–85.
18. Newton SC, Millette CF. Sertoli cell plasma membrane polypeptides involved in spermatogenic cell-Sertoli cell adhesion. J Androl 1992; 13:160–171.
19. Galdieri M, Zani B. Hormonal induced changes in Sertoli cell glycoproteins. Cell Biol Int Rep 1981; 5:111.
20. Neely MD, Boekelheide K. Sertoli cell processes have axoplasmic features: an ordered microtubule distribution and an abundant high molecular weight microtubule-associated protein (cytoplasmic dynein). J Cell Biol 1988; 107:1767–1776.
21. Pfister KK, Wagner MC, Bloom GS, Brady ST. Modification of the microtubule-binding and ATPase activities of kinesin by N-ethylmaleimide (NEM) suggests a role for sulfhydryls in fast axonal transport. Biochemistry 1989; 28:9006–9012.
22. Towbin H, Staehelin T, Gordon J. Electrophoretic transfer of proteins from polyacrylamide gels to nitrocellulose sheets: procedure and some applications. Proc Natl Acad Sci U S A 1979; 76:4350–4354.
23. Moore MS, Blobel G. The GTP-binding protein Ran/TC4 is required for protein import into the nucleus. Nature 1993; 365:661–663.
24. Kozak M. Point mutations define a sequence flanking the AUG initiator codon that modulates translation by eukaryotic ribosomes. Cell 1986; 44:283–292.
25. Nakagawa T, Tanaka Y, Matsuoka E, Kondo S, Okada Y, Noda Y, Kanai Y, Hirokawa N. Identification and classification of 16 new kinesin superfamily (KIF) proteins in mouse genome. Proc Natl Acad Sci U S A 1997; 94:9654–9659 [published erratum appears in Proc Natl Acad Sci U S A 1999; 96:4214].
26. Bairoch A, Bucher P, Hofmann K. The PROSITE database: its status in 1977. Nucleic Acids Res 1997; 25:217–221.
27. Murzin AG, Brenner SE, Hubbard T, Chothia C. SCOP: a structural classification of proteins database for the investigation of sequences and structures. J Mol Biol 1995; 247:536–540.
28. Ohtsubo M, Okazaki H, Nishimoto T. The RCC1 protein, a regulator for the onset of chromosome condensation locates in the nucleus and binds to DNA. J Cell Biol 1989; 109:1389–1397.
29. Patel R. Human DNA sequence from clone RP5-1043E3 on chromosome 6p21.1–21.2 contains part of a novel gene, a transcription factor E2F4 pseudogene, ESTs, STSs and GSSs. Bethesda, MD: GenBank National Center for Biotechnology Information, National Library of Medicine; 2000: accession no. AL36102.
30. Azuma Y, Dasso M. The role of Ran in nuclear function. Curr Opin Cell Biol 2000; 12:302–307.

31. Fleig U, Salus SS, Karig I, Sazer S. The fission yeast Ran GTPase is required for microtubule integrity. J Cell Biol 2000; 151:1101–1112.
32. Guarguaglini G, Renzi L, D'Ottavio F, Di Fiore B, Casenghi M, Cundari E, Lavia P. Regulated Ran-binding protein 1 activity is required for organization and function of the mitotic spindle in mammalian cells in vivo. Cell Growth Differ 2000; 11:455–465.
33. Cole A, Meistrich ML, Cherry LM, Trostle-Weige PK. Nuclear and manchette development in spermatids of normal and azh/azh mutant mice. Biol Reprod 1988; 38:385–401.
34. Meistrich ML, Trostle-Weige PK, Russell LD. Abnormal manchette development in spermatids of azh/azh mutant mice. Am J Anat 1990; 188:74–86.
35. Russell LD, Russell JA, MacGregor GR, Meistrich ML. Linkage of manchette microtubules to the nuclear envelope and observations of the role of the manchette in nuclear shaping during spermiogenesis in rodents. Am J Anat 1991; 192:97–120.
36. Walden PD, Cowan NJ. A novel 205-kilodalton testis-specific serine/threonine protein kinase associated with microtubules of the spermatid manchette. Mol Cell Biol 1993; 13:7625–7635.
37. Nakai M, Hess RA, Matsuo F, Gotoh Y, Nasu T. Further observations on carbendazim-induced abnormalities of spermatid morphology in rats. Tissue Cell 1997; 29:477–485.
38. Tanii I, Yoshinaga K, Toshimori K. The effects of brefeldin A on acrosome formation and protein transport to the acrosome in organ cultures of rat seminiferous tubules. J Electron Microsc (Tokyo) 1998; 47:161–167.
39. Moreno RD, Ramalho-Santos J, Sutovsky P, Chan EKL, Schatten G. Vesicular traffic and Golgi apparatus dynamics during mammalian spermatogenesis: implications for acrosome architecture. Biol Reprod 2000; 63:89–98.
40. Vogl AW, Pfeiffer DC, Mulholland D, Kimel G, Guttman J. Unique and multifunctional adhesion junctions in the testis: ectoplasmic specializations. Arch Histol Cytol 2000; 63:1–15.
41. Guttman JA, Kimel GH, Vogl AW. Dynein and plus-end microtubule-dependent motors are associated with specialized Sertoli cell junction plaques (ectoplasmic specializations). J Cell Sci 2000; 113:2167–2176.